

Supporting Information

Unprecedented Icosahedral Clusters Built of Polyantimony: From Single $[Ni_{0.5}@\{Sb_6Ni_6(CO)_8\}]^{4-}$ and $[Ni@\{Sb_7Ni_5(CO)_6\}]^{3-}$ to Sb_8^{4-} -linked Dimer $[(Sb_8)\{Sb_7Ni_5(CO)_4\}_2]^{6-}$

Lifang Lin, Shan Chen, Zhihao Lu, Li Xu*

Table of Contents

S1. Experimental Details

S2. Crystal structures

S3. EDX Spectroscopy and ICP results

S4. IR Spectroscopy

S5. Computational Methods and Details

S6. References

S1. Experimental Details

All manipulations were carried out under argon using standard Schlenk-line and glovebox techniques. The elements were loaded into quartz tubes in an argon atmosphere dry box and then sealed under vacuum. Melts of nominal composition of K₂ZnSb was prepared by fusion of stoichiometric ratios of the elements at high temperature (~1100 °C). The elements were loaded into quartz tubes in an argon atmosphere dry box and then sealed under vacuum. ¹ Ethylenediamine (Acros, 99%) was distilled over sodium metal and stored in a gastight Schlenk under argon in the glovebox. Toluene was dried with potassium-sodium alloy and then stored in the glovebox. 18-crown-6 (18-crown-6 = 1,4,7,10,13,16-hexaoxacyclooctadecane) (accela, 99%), PBu₄Br (Sigma-Aldrich, 99%), Ni(CO)₂(PPh₃)₂ (J&k Chemical, 99%).

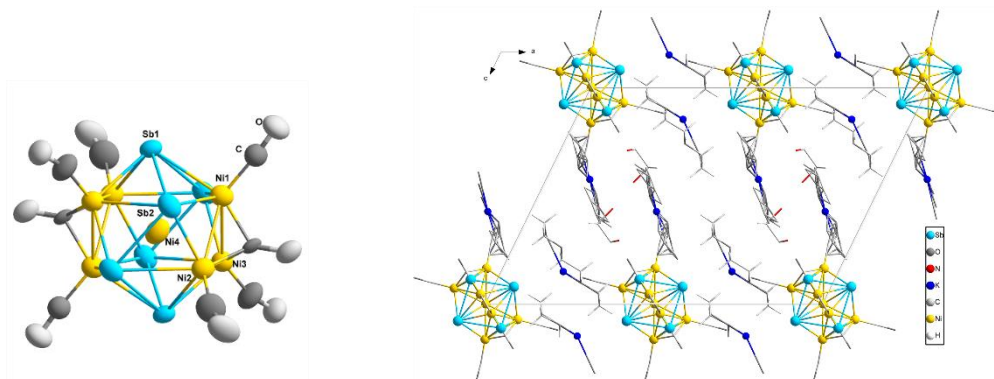
Synthesis of [K(18-crown-6)]₄[Ni_{0.5}@Sb₆Ni₆(CO)₈]·2en ([K(18-crown-6)]₄[1]·2en). K₂ZnSb (62 mg, 0.234 mmol), 18-crown-6 (100 mg, 0.378 mmol) were dissolved in en (~ 2mL) and stirred for 1h, resulting in a dark red solution. to which Ni(CO)₂(PPh₃)₂ (15 mg, 0.023 mmol) was added , yielding a red-brown solution. The resulting red-brown solution was heated at 60°C for 6h and filtered was filtered via a glass fiber pipette and the filtrate was layered with toluene (8 mL). Black, plate crystals of **1** (1.5 mg, 16.8% based on Ni) were obtained after a month.

Synthesis of [K(18-crown-6)]₃[Ni@Sb₇Ni₅(CO)₅] ([K(18-crown-6)]₃[2]). K₂ZnSb (62 mg, 0.234 mmol), 18-crown-6 (100 mg, 0.378 mmol) were dissolved in en (~ 2mL) and stirred for 1 h, resulting in a dark red solution. to which Ni(CO)₂(PPh₃)₂ (30 mg, 0.047 mmol) was added , yielding a red-brown solution. The resulting red-brown solution was heated at 65°C for 6h and filtered was filtered via a glass fiber pipette and the filtrate was layered with toluene (8 ml). Black, plate crystals of **2** (5 mg, 26.4% based on Ni) were obtained after three weeks.

Synthesis of [Bu₄P]₆[Sb₂₂Ni₁₀(CO)₈] ([Bu₄P]₆[3]). K₂ZnSb (62mg, 0.234mmol), Bu₄PBr (110 mg, 0.341 mmol) were dissolved in en (~ 2mL) and stirred for 1h, resulting in a dark red solution. to which Ni(CO)₂(PPh₃)₂ (10 mg, 0.016 mmol) was added , yielding a red-brown solution. The resulting red-brown solution was heated at 60°Cfor 6h and filtered was filtered via a glass fiber pipette and the filtrate was layered with toluene (8 mL). Black, plate crystals of **3** (2 mg, 23.0% based on Ni) were obtained after three weeks.

Synthesis of [K(18-crown-6)]₆[Sb₂₂Ni₁₀(CO)₈]·2toluene·3en([K(18-crown-6)]₆[4]·2toluene·3en). The synthesis of [K(18-crown-6)]₆[4]·2toluene·3en is basically the same as that of [Bu₄P]₆[3], except that Bu₄PBr is replaced by 18-crown-6. Black, plate crystals of **4** (2 mg, 23.6% based on Ni) were obtained after a month and a half.

S2. Crystal structures



a

b

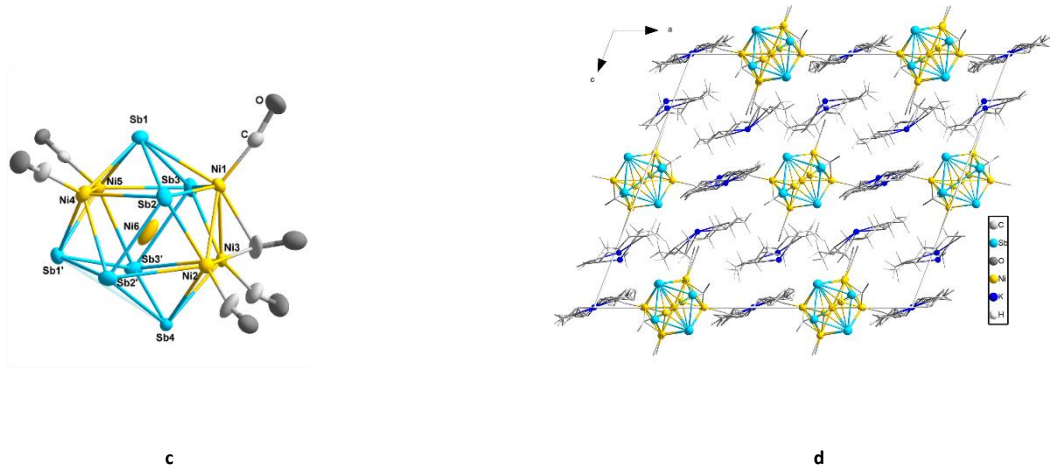


Figure S1. (a) the structure of the cluster **1** displacement ellipsoids with 30% probability; (b) the crystal structure of **1** down b axis; (c) the structure of the cluster **2** displacement ellipsoids with 30% probability; (d) the crystal structure of **2** down b axis.

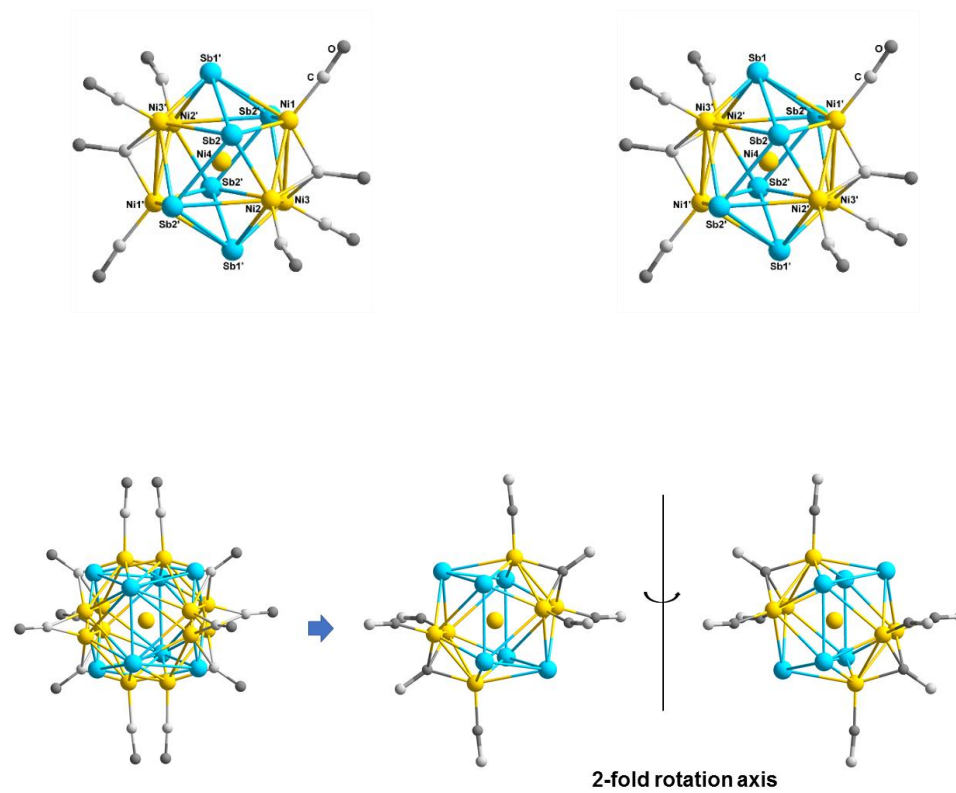


Figure S2. An additional pseudo 2-fold axis within the crystallographic mirror plane of the disordered structure of **1**.

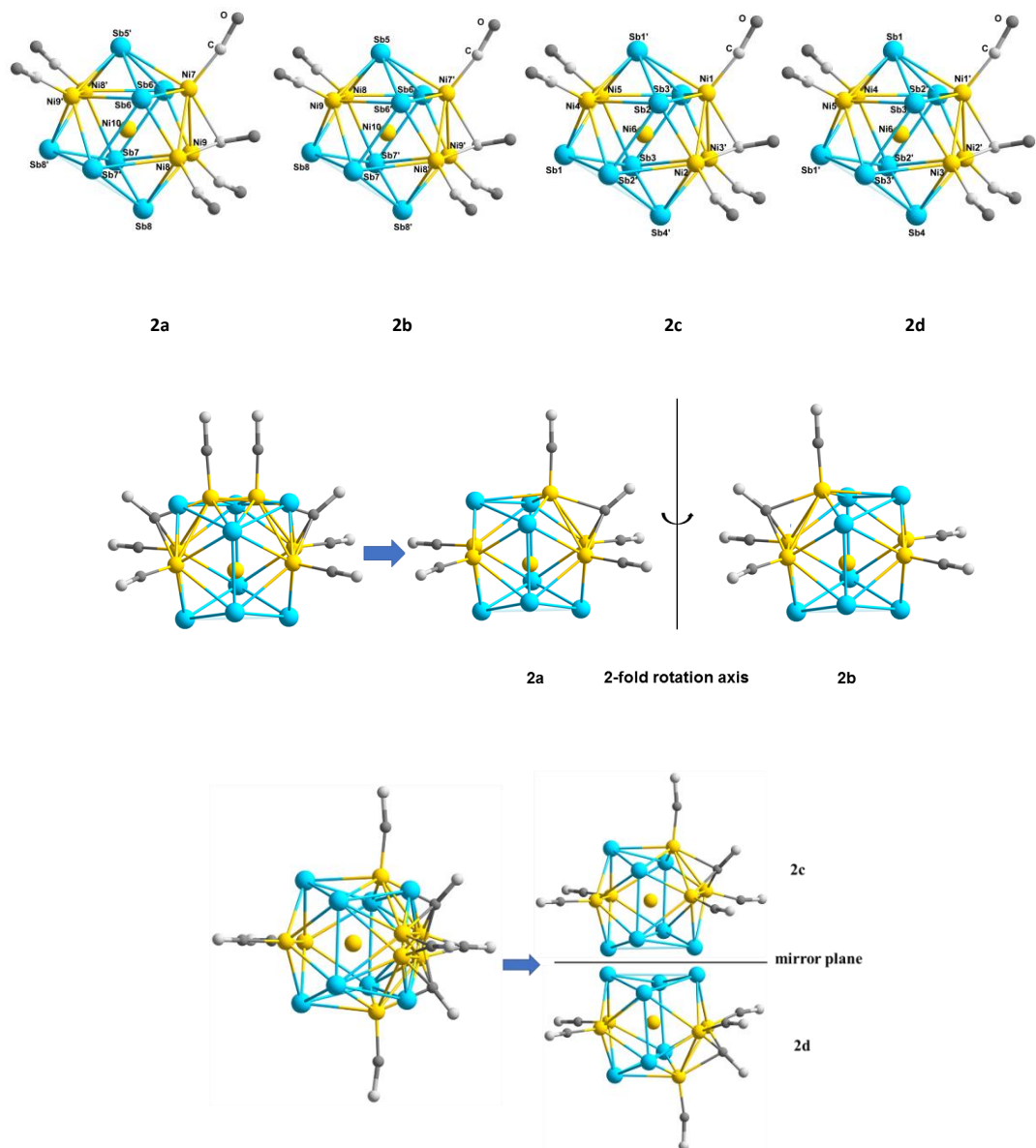
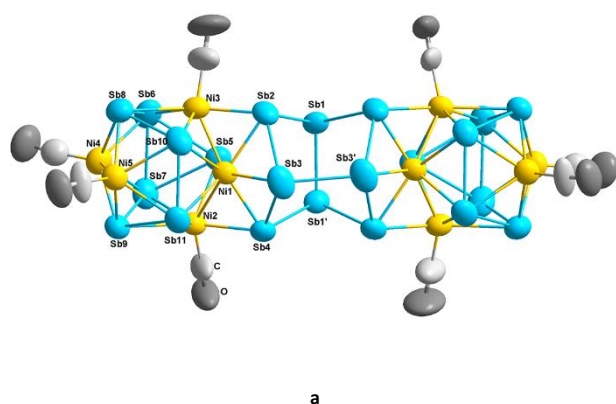


Figure S3. An additional pseudo 2-fold axis and the crystallographic mirror plane of the disordered structure of **2**.



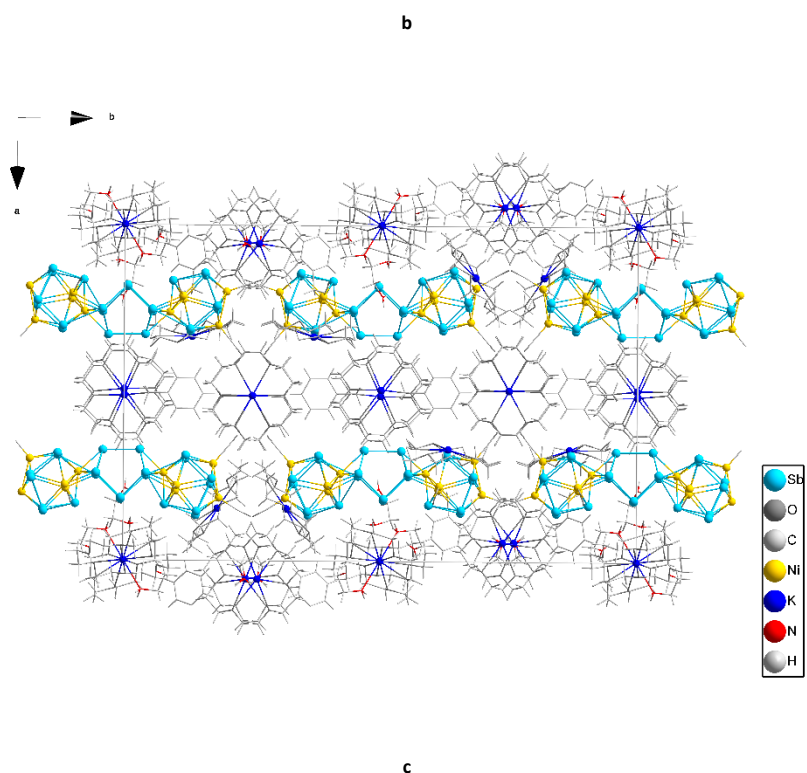
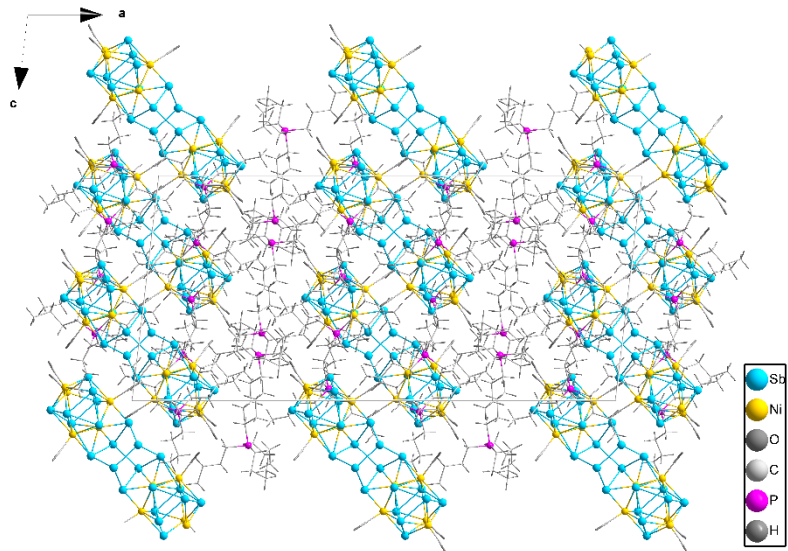


Figure S4. The structure of the cluster **3/4** displacement ellipsoids with 30% probability (a); the crystal structure of $[Bu_4P]_6[3]/[K(18\text{-crown}\text{-}6)]_6[4]\cdot 2\text{toluene}\text{-}3\text{en}$ down *b* and *c* axis, respectively (b and c).

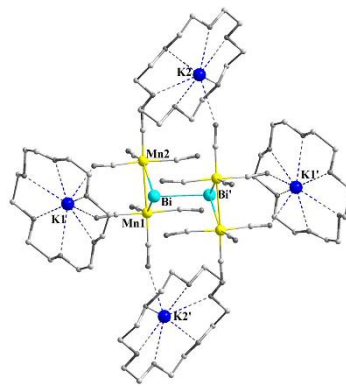


Figure S5. The structure of $\left[\left[\text{K}(18\text{-crown-6})\right]_2\{[(\text{CO})_4\text{Mn}]_2(\mu_2\text{-Bi})\}\right]$

Table S1. Table 1. Sb-Sb bond lengths in Sb_n anions (\AA)

Sb_n	Sb-Sb	Sb-Sb(av.)	Δ (range)
$[\text{Sb}_4]^{2-\text{a}}$	2.749(1) – 2.751(1)	2.750	0.002
$[\text{Sb}_5]^{5-\text{b}}$	2.8059(10) – 2.9103(10)	2.849	0.1044
$[\text{Sb}_6(\text{RuCp})_2]^{2-\text{c}}$	2.7324(2) – 2.9538(2)	2.83	0.2214
$[\text{Ni}_{0.5}@\{\text{Sb}_6\text{Ni}_6(\text{CO})_8\}]^{4-\text{(1)}}$	2.8716(14) – 3.0250(17)	2.948	0.1534
$[\text{Ni}@\{\text{Sb}_7\text{Ni}_5(\text{CO})_6\}]^{3-\text{(2)}}$	2.897(3) – 3.064(3)	3.004	0.167
$[\text{Sb}_7]^{3-\text{d}}$	2.711(4) – 2.906(2)	2.820	0.195
$[\text{Sb}_7\text{Ni}_5(\text{CO})_4]^- \text{(3a)}$	2.837(3) – 2.980(2)	2.890	0.143
$[\text{Sb}_7\text{Ni}_5(\text{CO})_4]^- \text{(4a)}$	2.857(4) – 2.977(4)	2.905	0.120
$\text{Sb}_8^{4-\text{(3)}}$	2.814(3)-2.943(5)	2.866	0.129
$\text{Sb}_8^{4-\text{(4)}}$	2.795(4)- 2.919(4)	2.874	0.124
$[\text{Sb}_8]^{8-\text{e}}$	2.847(2) – 2.872(3)	2.861	0.025
$[(\text{Cp}^*\text{Sm})_4\text{Sb}_8]^\text{f}$	2.7938(7)- 2.8559(8)	2.8249	0.062
$[\text{Sb}_{10}]^{2-\text{g}}$	2.673(2) – 2.851(3)	2.743	0.178
$[\text{Sb}_{11}]^{3-\text{h}}$	2.716(4) – 2.853(4)	2.803	0.137

a Ref. 32c. b Ref. 32e. c Ref. 31. d 2. e Ref. 29. f Ref. 33. g 4.

Table S2. Bond lengths [\AA] for **1**, **2**, **3**, **4**, $[\text{Sb}_7\text{Ni}_3(\text{CO})_3]^{3-}$ and $[\text{Sb}_3\text{Ni}_4(\text{CO})_6]^{3-}$, as well as $[\text{Ni}_3(\text{i-Pr}_2\text{Im})_3(\mu_2\text{-CO})_3(\mu_3\text{-CO})]$. “ Ni_c ” is for the central Ni atom.

Bond	1	2	3/4	$[\text{Sb}_7\text{Ni}_3(\text{CO})_3]^{3-\text{a}}$	$[\text{Sb}_3\text{Ni}_4(\text{CO})_6]^{3-\text{b}}$	$[\text{Ni}_3(\text{i-Pr}_2\text{Im})_3(\mu_2\text{-CO})_3(\mu_3\text{-CO})]^\text{c}$
Sb-Sb	2.8716(1),3.0250(17)	2.897(3)-3.064(3)	2.814(3)-2.956(3)/ 2.795(4)-2.977(4)	2.810(8)-2.977(8)	2.851(2) -2.873(4)	-
	av. 2.9483	av. 2.981	av. 2.882/2.890	av. 2.888	av. 2.862	-
Sb-Ni	2.457(3)-2.769(4)	2.503(5)-2.921(5)	2.484(3)- 2.815(5)/ 2.506(5)-2.825(6)	2.51(1)- 2.71(1)	2.550(3)- 2.864(5)	-
	av. 2.594	av. 2.650	av. 2.625/2.629	av. 2.57	av. 2.673	-

Sb ₈ ⁴⁻ -Ni	-	-	2.520(4)-2.653(4)/ 2.552(5)-2.638(5)	-	-	-
Ni-Ni	2.603(5), 2.605(5)	2.596(7)-2.789(6)	av.2.529/2.601 2.593(5)-2.717(5)/ 2.623(7)-2.745(7)	2.68(1), 2.79(1)	2.332(6)- 2.568(4)	2.3582(6)-2.3663(6)
	av. 2.604	av. 2.664	av. 2.655/2.684	av. 2.735	av. 2.414	av. 2.3623
Sb-Ni _c	2.6701(6),2.6755(1)	2.728(4)-2.756(3)	-	-	-	-
	av. 2.6728	av. 2.735	-	-	-	-
Ni-Ni _c	2.443(4), 2.468(3)	2.465(6)-2.488(5)	-	-	-	-
	av. 2.456	av. 2.477	-	-	-	-

a Ref. 28. b Ref. 23. c Ref. 30.

S3. EDX Spectroscopy and ICP results

The energy-dispersive X-ray spectroscopy (EDX, JEOLSEM, JSM-6700F) analyses of the single crystals of [K(18-crown-6)]₄ [1]·2en, [K(18-crown-6)]₃ [2], [Bu₄P]₆[3], [K(18-crown-6)]₆[4] ·2toluene·3en; Combustion analyses, namely Inductively Coupled Plasma Optical Emission Spectroscopy (ICP-OES) analyses of the crystalline samples were also carried on Ultima 2. The ICP results are close to both calculated and EDX values and hence provide additional evidence of the sample purity in addition to X-ray analyses.

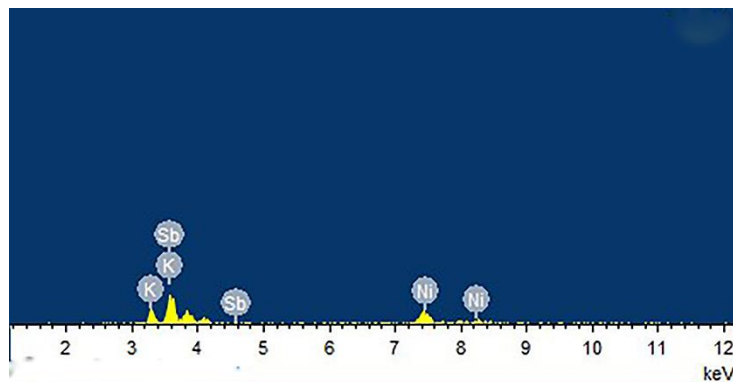


Figure S6. EDX analysis of [K(18-crown-6)]₄[Ni_{0.5}@Sb₆Ni₆(CO)₈]·2en ([K(18-crown-6)]₄ [1]·2en)

Element	Weight %	Atom %	Ratio(exp)	Ratio (cal)
K	11.87	22.82	3.8	4
Ni	34.35	43.98	7.3	6.5
Sb	53.77	33.20	5.5	6

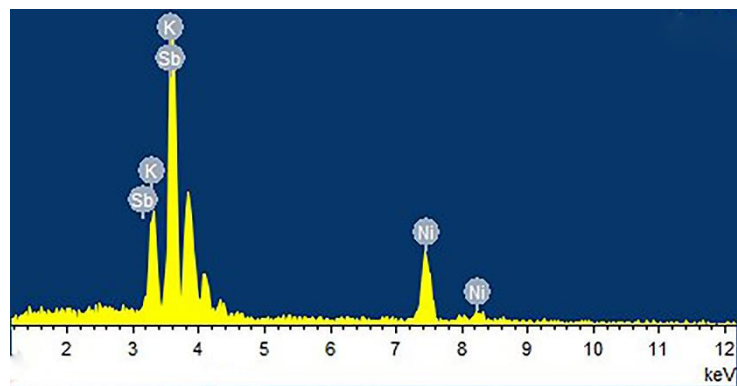


Figure S7. EDX analysis of $[K(18\text{-crown}\text{-}6)]_3[Ni@Sb_7Ni_5(CO)_5]$ ($[K(18\text{-crown}\text{-}6)]_3[2]$)

Element	Weight %	Atom %	Ratio(exp)	Ratio (cal)
K	8.71	19.10	3.2	3
Ni	21.98	32.10	5.5	6
Sb	69.31	48.80	8.3	7

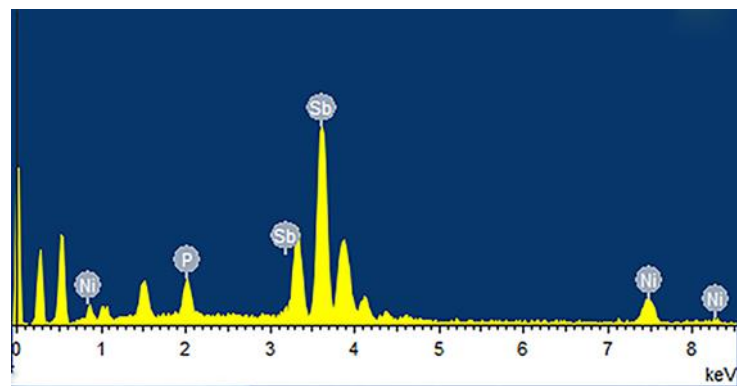


Figure S8. EDX analysis of $[PBu_4]_6[Sb_{22}Ni_{10}(CO)_8]$ ($[Bu_4P]_6[3]$)

Element	Weight %	Atom %	Ratio(exp)	Ratio (cal)
P	4.95	59.41	5.7	6
Ni	16.50	25.88	9.8	10
Sb	78.55	14.71	22.8	22

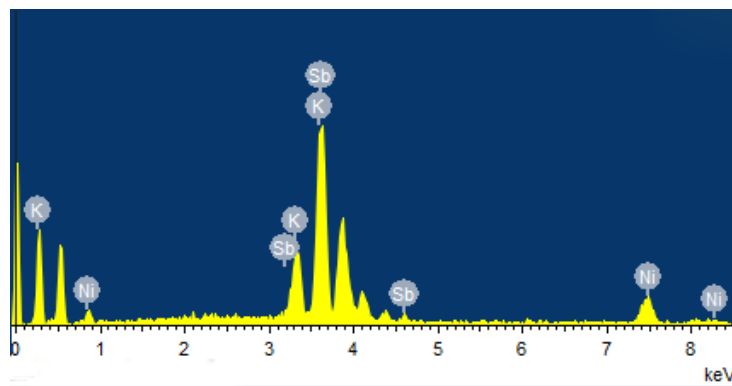


Figure S9. EDX analysis of $[K(18\text{-crown}\text{-}6)]_6[Sb_{22}Ni_{10}(CO)_8]\cdot 2\text{toluene}\cdot 3\text{en}$ ($[K(18\text{-crown}\text{-}6)]_6[4]\cdot 2\text{toluene}\cdot 3\text{en}$)

Element	Weight %	Atom %	Ratio(exp)	Ratio (cal)
K	5.77	14.07	5.5	6
Ni	14.38	23.36	9.1	10
Sb	79.86	62.57	24.5	22

Table S3. ICP result of $[K(18\text{-crown}\text{-}6)]_4[1]\cdot 2\text{en}$.

Element	Measured mg/L	Weight %	Cal. Weight %
K	2.77	17.65	12.33
Ni	3.09	19.51	30.07
Sb	9.83	62.65	57.59

Table S4. ICP result of $[K(18\text{-crown}\text{-}6)]_3[2]$.

Element	Measured mg/L	Weight %	Cal. Weight %
K	15.75	8.32	8.87
Ni	52.93	27.93	26.64
Sb	120.63	63.72	64.48

Table S5. ICP result of $[Bu_4P]_6[3]$.

Element	Measured mg/L	Weight %	Cal. Weight %
Sb	18.86	80.77	82.06
Ni	4.49	19.23	17.97

S4. IR Spectroscopy

The IR spectra of $[K(18\text{-crown}\text{-}6)]_4$ [1]·2en, $[K(18\text{-crown}\text{-}6)]_3$ [2] and $[Bu_4P]_6$ [3] were recorded as KBr pellets in Nujol mulls on a Magna 750 FT-IR spectrometer photometer.

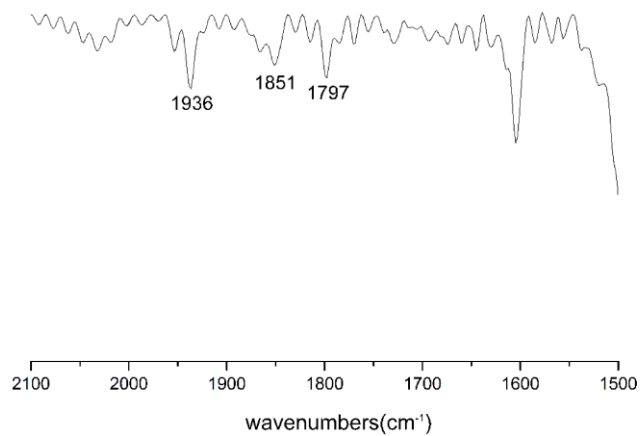


Figure S10. The IR spectrum of $[K(18\text{-crown}\text{-}6)]_4$ [1]·2en.

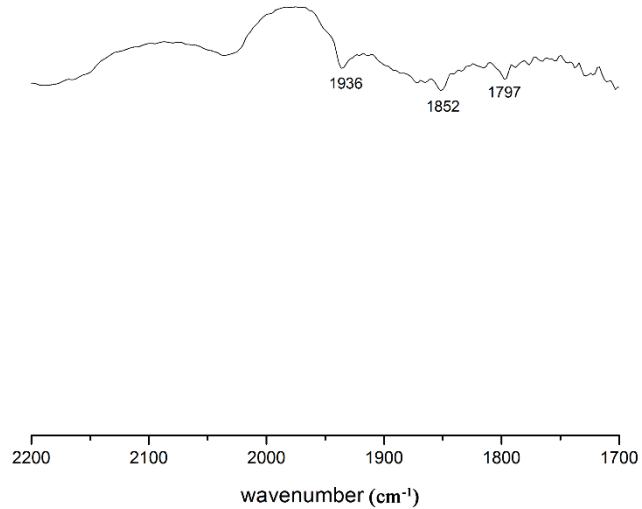


Figure S11. The IR spectrum of $[K(18\text{-crown}\text{-}6)]_3$ [2].

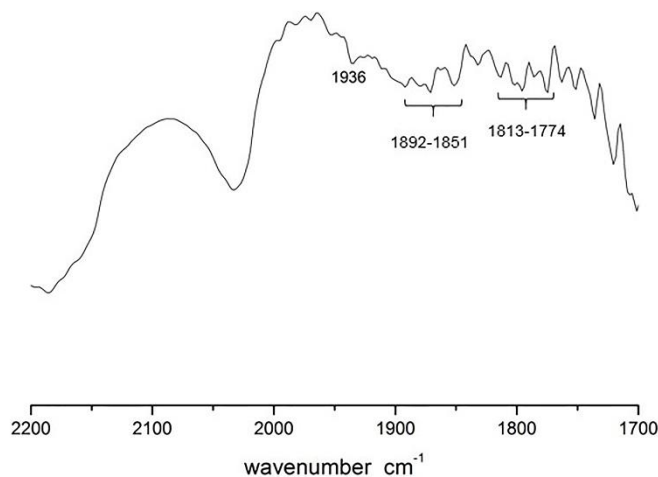


Figure S12. The IR spectrum of $[\text{Bu}_4\text{P}]_6[\mathbf{3}]$.

S5. Computational Methods and Details

All calculations on experimental structures of anions **1- 3** were performed using Gaussian 09 program⁵ at the B3LYP/ LanL2DZ level of theory.⁶ In these calculations, the solvent effects were taken into account by polarizable continuum model (PCM)⁷. natural population analysis (NPA)⁸ on clusters **1-3** were carried out by using Multiwfn⁹ and the results were presented in Table S6. To clarify the chemical bonding patterns of **1-3**, we calculated the Mayer/Fuzzy bond orders¹⁰ (Table S7). We performed the charge decomposition analysis (CDA)¹¹ using Multiwfn,⁹ which is a multifunctional wave function analysis program using the files generated from the Gaussian calculations. Results of these analyses were summarized in Table S8. Figure S13 pointed out the occurrence of electron transfer from the Sb_8^{4-} anions to the $[\text{Sb}_7\text{Ni}_5(\text{CO})_4]^-$ fragments. And also performed the Adaptive Natural Density Partitioning analyses¹² (Figure S14-23) on the experimental structures by using Multiwfn.⁹ The Sb and Ni atoms are defined in Figure S1 and S4.

Table S6. Natural Population Analysis (NPA) of **1-3**.

(a) Cluster anion **1a**

Atom	Charge
Sb1	0.349
Sb1'	0.349
Sb2	0.358
Sb2'	0.356
Ni1	-1.00
Ni2	-0.903
Ni3	-0.957

Ni4	-1.153
(b) Cluster anion 1b	
Atom	Charge
Sb1	0.287
Sb1'	0.287
Sb2	0.304
Sb2'	0.299
Ni1	-1.080
Ni2	-1.016
Ni3	-1.01
(c) Cluster anion 2	
Atom	Charge
Sb1	0.485
Sb1'	0.333
Sb2	0.382
Sb3	0.369
Sb4	0.516
Ni1	-1.061
Ni2	-0.975
Ni3	-0.939
Ni4	-1.051
Ni5	-1.061
Ni6	-1.143
(d) Cluster anion 3	
Atom	Charge
Sb1	-0.167
Sb1'	-0.167
Sb2	0.338

Sb3	0.032
Sb3'	0.033
Sb4	0.337
Sb5	0.436
Sb6	0.258
Sb7	0.254
Sb8	0.306
Sb9	0.313
Sb10	0.327
Sb11	0.328
Ni1	-1.430
Ni2	-1.170
Ni3	-1.164
Ni4	-1.218
Ni5	-1.118

Table S7. Distances, MBOs, and FBOs of the short Sb-Sb, Sb-Ni and Ni-Ni bonds in the heterometallic cluster ions **1-3**.

(a) Cluster anion 1			
Bond	Distances(Å)	MBO	FBO
Sb1-Sb2	3.0250(17)	0.46	0.61
Sb2-Sb2'	2.8716(14)	0.52	0.72
Sb1-Ni1	2.769(4)	0.40	0.50
Sb1-Ni2	2.625(3)	0.35	0.57
Sb1-Ni3	2.628(3)	0.34	0.57
Sb1-Ni4	2.6755(15)	0.49	0.48
Sb2-Ni1	2.520(3)	0.44	0.63
Sb2-Ni2	2.457(3)	0.52	0.74

Sb2'-Ni2	2.959(3)	0.20	0.37
Sb2'-Ni3	2.465(3)	0.52	0.74
Sb2-Ni3'	2.939(3)	0.18	0.35
Sb2-Ni4	2.6701(6)	0.47	0.45
Ni1-Ni2	2.605(5)	0.29	0.35
Ni1-Ni3	2.616(5)	0.28	0.35
Ni1-Ni4	2.443(4)	N	0.37
Ni2-Ni3	2.603(5)	0.28	0.37
Ni2-Ni4	2.468(3)	N	0.36
Ni3-Ni4	2.474(3)	N	0.36

(b) Cluster anion **2**

Bond	Distances(Å)	MBO	FBO
Sb1-Sb2	3.018(2)	0.37	0.55
Sb1'-Sb2	3.040(3)	0.44	0.65
Sb2-Sb2'	2.897(3)	0.52	0.73
Sb1'-Sb2	3.064(3)	0.42	0.65
Sb3-Sb3'	2.891(3)	0.52	0.71
Sb1-Ni1	2.688(6)	0.46	0.57
Sb1-Ni4	2.540(3)	0.55	0.69
Sb1-Ni6	2.756(3)	0.31	0.37
Sb2'-Ni1	2.614(6)	0.37	0.56
Sb2'-Ni2	2.503(5)	0.61	0.66
Sb2'-Ni4	2.698(4)	0.43	0.57
Sb2'-Ni6	2.728(4)	0.22	0.39

Sb2-Ni4	2.921(5)	0.33	0.37
Sb2-Ni4	2.710(3)	0.35	0.56
Sb2-Ni6	2.737(4)	0.50	0.49
Sb4-Ni2	2.624(5)	0.45	0.55
Sb4-Ni6	2.721(4)	0.62	0.53
Sb1'-Ni3	2.548(3)	0.49	0.70
Sb1'-Ni4	2.756(3)	0.64	0.49
Ni1-Ni2	2.606(7)	0.22	0.37
Ni1-Ni6	2.488(5)	0.11	0.36
Ni2-Ni3	2.596(7)	0.21	0.36
Ni2-Ni6	2.486(7)	N	0.37
Ni4-Ni5	2.789(6)	0.43	0.30
Ni4-Ni6	2.465(6)	N	0.37

(b) Cluster anion **3**

Bond	Distances(Å)	MBO	FBO
Sb1-Sb1'	2.814(3)	0.83	1.02
Sb1-Sb2	2.863(2)	0.78	0.94
Sb2-Sb3	2.891(3)	0.61	0.80
Sb3-Sb3'	2.953(4)	0.69	0.92
Sb5-Sb6	2.956(3)	0.47	0.67
Sb6-Sb7	2.885(3)	0.45	0.75
Sb6-Sb8	2.880(4)	0.45	0.70
Sb8-Sb9	2.852(3)	0.54	0.76
Sb8-Sb10	2.837(3)	0.54	0.77

Sb10-Sb11	2.876(4)	0.54	0.75
Sb2 -Ni1	2.561(4)	0.54	0.63
Sb3-Ni1	2.625(4)	0.59	0.61
Sb5-Ni1	2.484(3)	0.42	0.65
Sb5-Ni2	2.620(4)	0.54	0.60
Sb6-Ni2	2.605(5)	0.57	0.65
Sb6-Ni4	2.614(5)	0.50	0.65
Sb8-Ni2	2.815(5)	0.45	0.49
Sb8-Ni4	2.552(5)	0.57	0.71
Sb10-Ni1	2.579(4)	0.61	0.62
Sb10-Ni2	2.669(4)	0.43	0.55
Sb10-Ni5	2.689(4)	0.45	0.59
Ni1-Ni2	2.682(4)	0.26	0.38
Ni4-Ni5	2.717(5)	0.37	0.37

Table S8. Results of the charge decomposition analysis (CDA) on the cluster ion **3**

Orbital	Occupancy	Donation	Back donation	Charge polarization
HOMO-41	2.00	0.048	0.006	-0.043
HOMO-35	2.00	0.015	0.002	-0.012
HOMO-34	2.00	0.013	-0.003	-0.062
HOMO-31	2.00	0.036	0.008	-0.092
HOMO-28	2.00	0.022	-0.001	-0.062
HOMO-27	2.00	0.023	0.005	-0.028
HOMO-23	2.00	0.011	-0.003	0.053
HOMO-22	2.00	0.042	0.001	-0.122
HOMO-21	2.00	0.021	0.003	-0.048
HOMO-18	2.00	0.066	0.009	-0.160
HOMO-17	2.00	0.026	-0.002	0.017
HOMO-16	2.00	0.025	0.000	-0.060

HOMO-15	2.00	0.040	0.002	-0.072
HOMO-14	2.00	0.035	0.009	-0.105
HOMO-13	2.00	0.023	0.017	-0.060
HOMO-11	2.00	0.033	0.020	0.079
HOMO-9	2.00	0.027	0.016	-0.111
HOMO-8	2.00	0.039	0.010	-0.141
HOMO-6	2.00	0.021	0.006	-0.129
HOMO-5	2.00	0.024	0.004	-0.116
HOMO-1	2.00	0.000	0.015	-0.243
HOMO	2.00	-0.006	0.017	-0.374

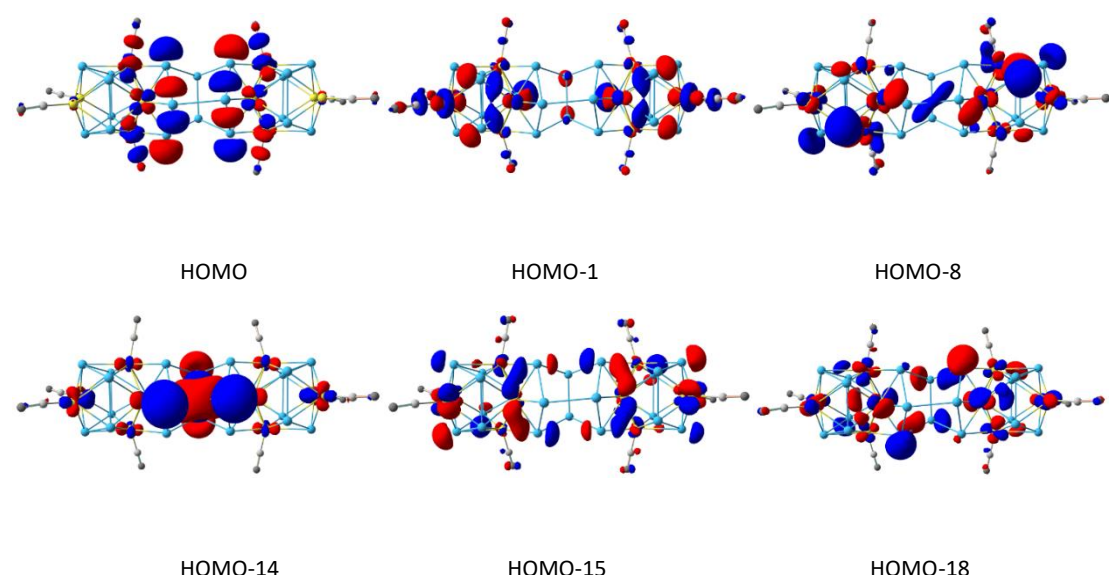
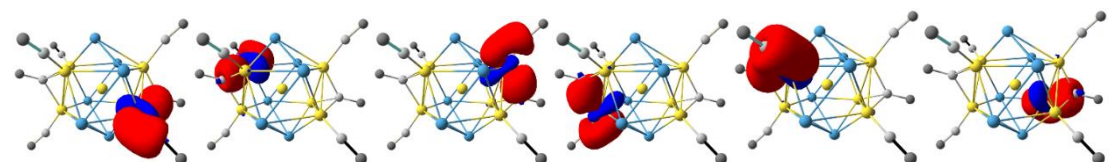


Figure S13. Representative occupied molecular orbitals of the anion **3a**. HOMO, HOMO-1 orbitals contribute to the electron back-donation from the $[\text{Sb}_2\text{Ni}_5]^-$ to the Sb_8^{4-} . HOMO-8, HOMO-14, HOMO-15, HOMO-18 orbitals contribute to the electron donation from the Sb_8^{4-} to the $[\text{Sb}_2\text{Ni}_5]^-$.

The chemical bonding patterns of the anion **1a**, where the legends “c”, “e”, and “ON” refer to “center”, “electron”, and “occupation number”, respectively.



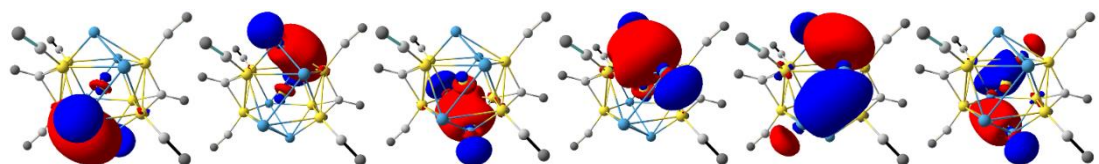


Figure S14. Twelve 3c-2e bonds ON = 1.93–1.71 | e |

The chemical bonding patterns of the anion 2a, where the legends “c”, “e”, and “ON” refer to “center”, “electron”, and “occupation number”, respectively.

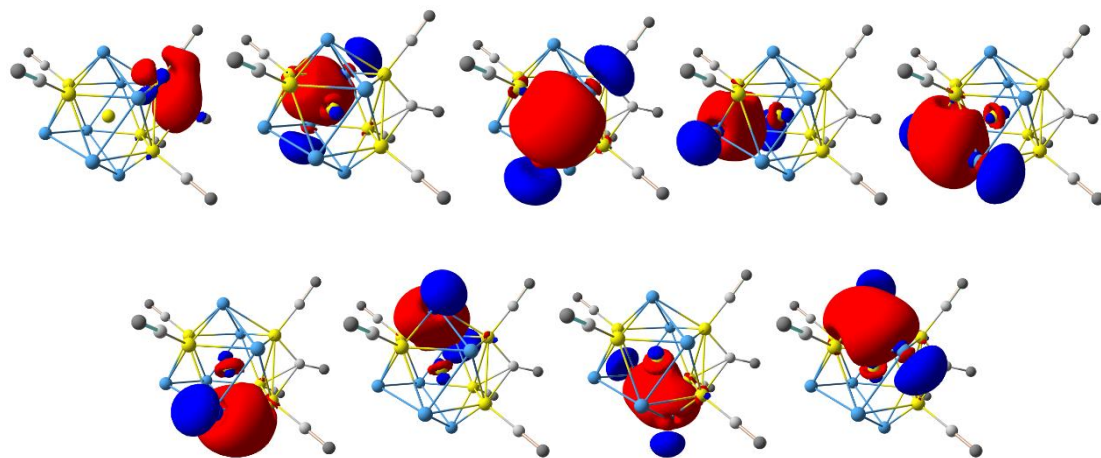


Figure S15. Nine 3c-2e bonds ON = 1.94–1.72 | e |

The chemical bonding patterns of Sb₈, where the legends “c”, “e”, and “ON” refer to “center”, “electron”, and “occupation number”, respectively.

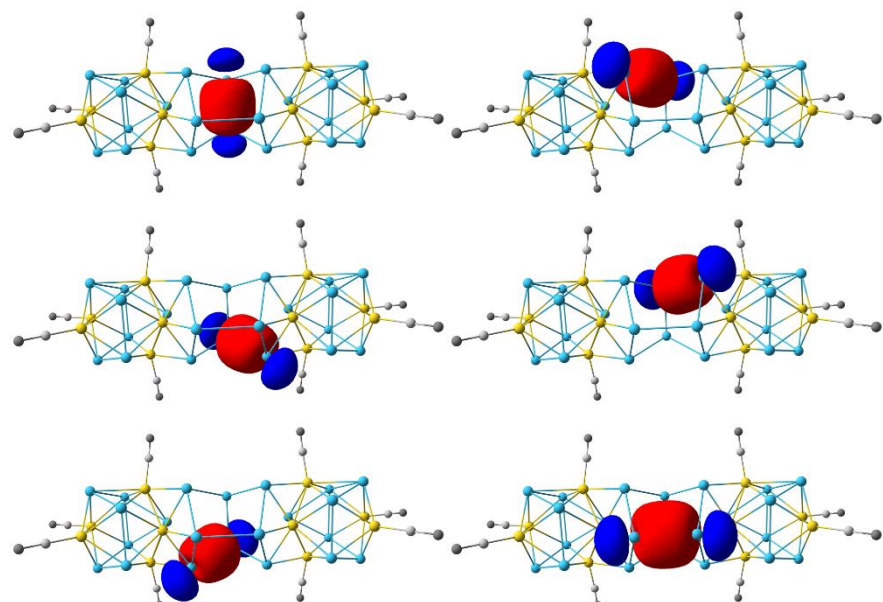


Figure S16. Six 2c-2e bonds ON = 1.97–1.91 | e |

The chemical bonding patterns between Sb_8 and $\text{Sb}_7\text{Ni}_5(\text{CO})_4$, where the legends “c”, “e”, and “ON” refer to “center”, “electron”, and “occupation number”, respectively.

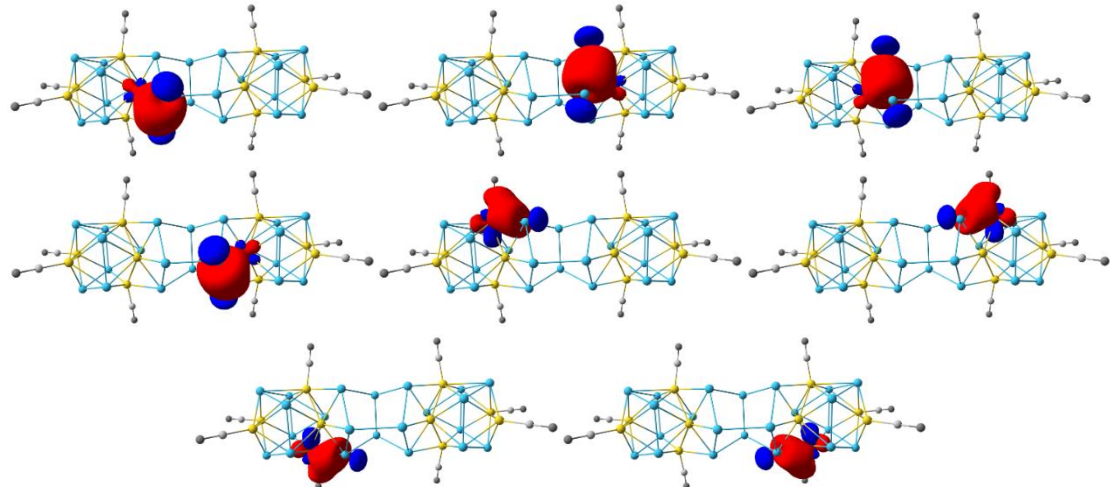


Figure S17. Eight 3c-2e bonds ON = 1.96–1.92 | e |

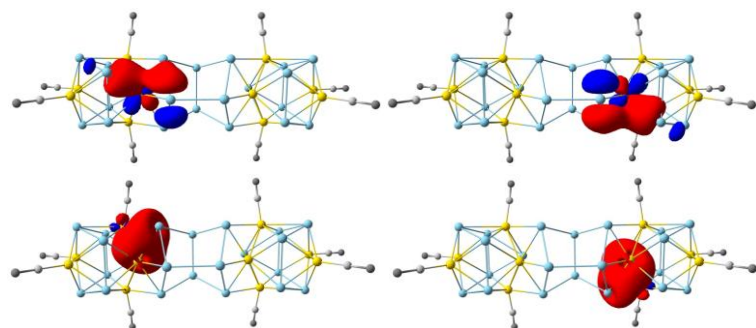


Figure S18. Four 4c-2e bonds ON = 1.87–1.77 | e |

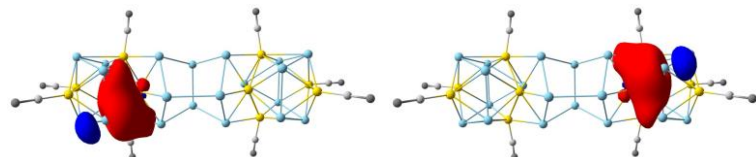


Figure S19. Two 5c-2e bonds ON = 1.79 | e |

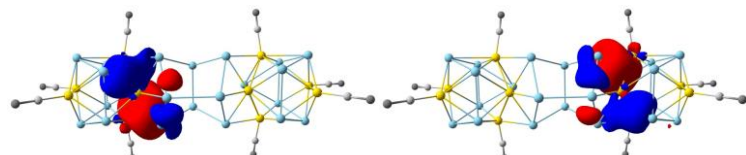


Figure S20. Two 7c-2e bonds ON = 1.77 | e |

The chemical bonding patterns of $\text{Sb}_7\text{Ni}_5(\text{CO})_4$, where the legends “c”, “e”, and “ON” refer to “center”, “electron”, and “occupation number”, respectively.

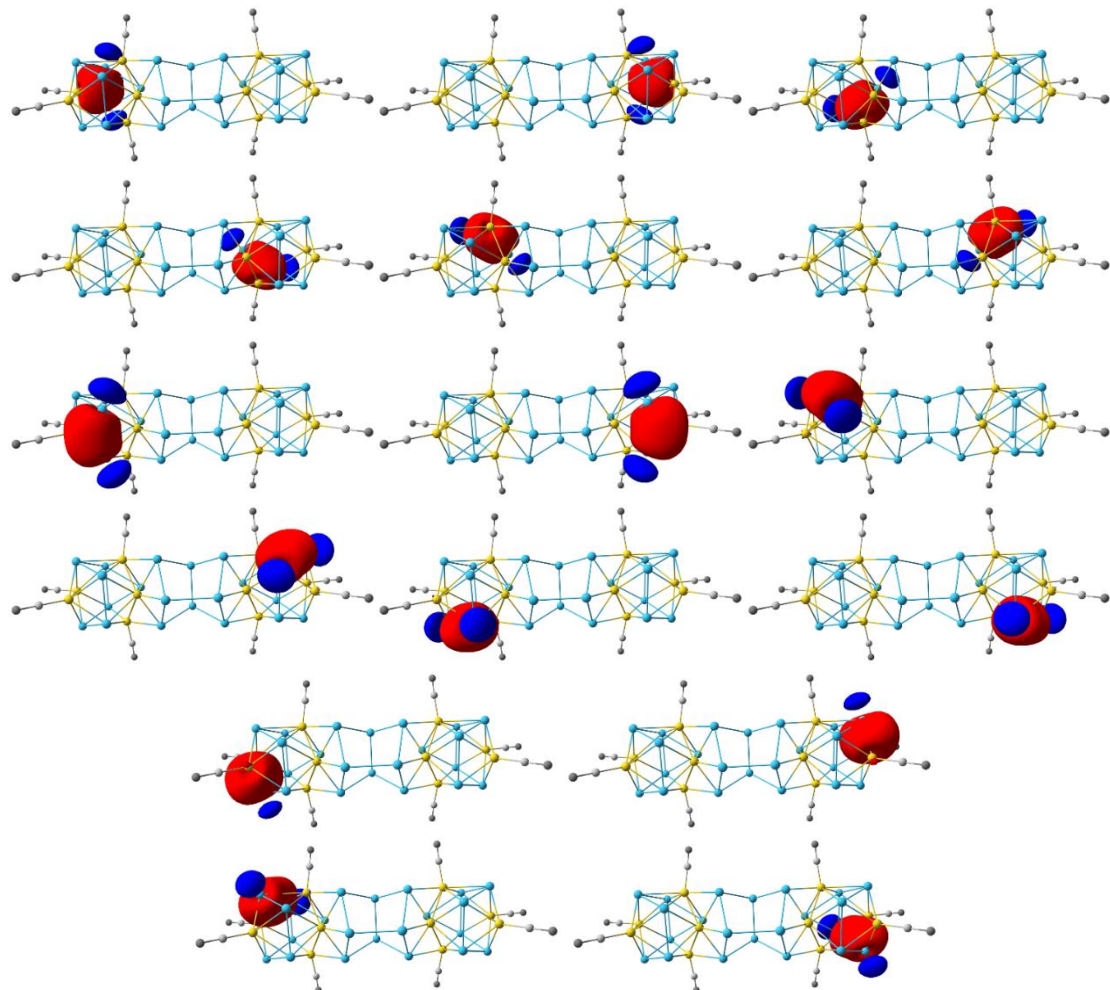


Figure S21. Sixteen 3c-2e bonds ON = 1.94–1.82 | e |

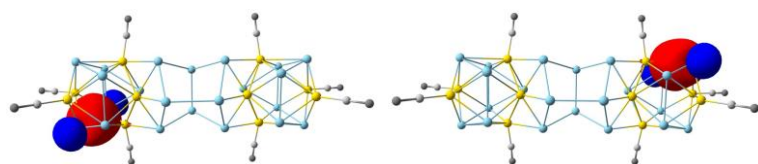


Figure S22. Two 4c-2e bonds ON = 1.83 | e |

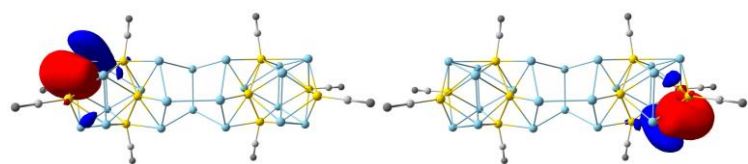


Figure S23. Two 6c-2e bonds ON = 1.74 | e |

S6. References

- 1 Y. Wang, M. Moses-DeBusk, L. Stevens, J. Hu, P. Zavalij, K. Bowen, B. I. Dunlap, E. R. Glaser and B. Eichhorn, Sb@Ni12@Sb20-/+ and Sb@Pd12@Sb20n Cluster Anions, Where n = +1,-1, -3, -4: Multi-Oxidation-State Clusters of Interpenetrating Platonic Solids, *J. Am. Chem. Soc.*, 2017, **139**, 619-622.
- 2 H. J. Breunig, M. E. Ghesner and E. Lork, Syntheses of the Antimonides R₂Sb⁻ (R= Ph, Mes, tBu, tBu₂Sb) and Sb₇³⁻ by Reactions of Organoantimony Hydrides or cyclo-(tBuSb)₄ with Li, Na, K, or BuLi, *Z. Anorg. Allg. Chem.*, 2005, **631**, 851-856.
- 3 H. Ruan, L. Wang, Z. Li and L. Xu, Sb₁₀²⁻ and Sb₂²⁻ found in [K(18-crown-6)]₆[Sb₁₀] [Sb₄{Mo(CO)₃}₂]⁻·2en: two missing family members, *Dalton Trans.*, 2017, **46**, 7219-7222.
- 4 (a) U. Bolle and W. Tremel, [Na(2,2,2-crypt)]₃[Sb₁₁], a Salt Containing the Undecaantimonide(3-) Anion, *J. Am. Chem. Soc. Commun.*, 1992, **91**; (b) T. Hanauer and N. Korber, [Sb₁₁]³⁻ and [As₁₁]³⁻: Synthesis and Crystal Structure of Two New Ammoniates containing Trishomocubane-like Polyanions, *Z. Anorg. Allg. Chem.*, 2006, **632**, 1135-1140.
- 5 Gaussian 09, Revision A.1, M. J. Frisch, G. W. Trucks, H. B. Schlegel, G. E. Scuseria, M. A. Robb, J. R. Cheeseman, G. Scalmani, V. Barone, G. A. Petersson, H. Nakatsuji, X. Li, M. Caricato, A. Marenich, J. Bloino, B. G. Janesko, R. Gomperts, B. Mennucci, H. P. Hratchian, J. V. Ortiz, A. F. Izmaylov, J. L. Sonnenberg, D. Williams-Young, F. Ding, F. Lipparini, F. Egidi, J. Goings, B. Peng, A. Petrone, T. Henderson, D. Ranasinghe, V. G. Zakrzewski, J. Gao, N. Rega, G. Zheng, W. Liang, M. Hada, M. Ehara, K. Toyota, R. Fukuda, J. Hasegawa, M. Ishida, T. Nakajima, Y. Honda, O. Kitao, H. Nakai, T. Vreven, K. Throssell, J. A. Montgomery, Jr., J. E. Peralta, F. Ogliaro, M. Bearpark, J. J. Heyd, E. Brothers, K. N. Kudin, V. N. Staroverov, T. Keith, R. Kobayashi, J. Normand, K. Raghavachari, A. Rendell, J. C. Burant, S. S. Iyengar, J. Tomasi, M. Cossi, J. M. Millam, M. Klene, C. Adamo, R. Cammi, J. W. Ochterski, R. L. Martin, K. Morokuma, O. Farkas, J. B. Foresman, and D. J. Fox, Gaussian, Inc., Wallingford CT, 2009.
- 6 J. H. Enemark, L. B. Friedman and W. N. Lipscomb, The Molecular and Crystal Structure of B₂₀H₁₆(NCCH₃)₂·CH₃CN, *Inorg. Chem.*, 1966, **5**, 2165-2172.
- 7 S. Miertu, E. Scrocco and J. Tomasi, Electrostatic interaction of a solute with a continuum. A direct utilization of AB initio molecular potentials for the revision of solvent effects, *Chem. Phys.*, 1981, **55**, 117-129.
- 8 A. E. Reed, R. B. Weinstock and F. Weinhold, Natural population analysis, *J. Chem. Phys.*, 1985, **83**, 735 – 746.
- 9 T. Lu and F. Chen, Multiwfns: A multifunctional wavefunction analyser, *J. Comput. Chem.*, 2012, **33**, 580-592.
- 10 (a) I. Mayer and P. Salvador, Overlap populations, bond orders and valences for 'fuzzy' atoms, *Chem. Phys. Lett.*, 2004, **383**, 368-375. (b) I. Mayer, Charge, bond order and valence in the ab initio SCF theory, *Chem. Phys. Lett.*, 1983, **97**, 270-274.
- 11 S. Dapprich and G. Frenking, A Charge Decomposition Analysis Using Fragment Molecular Orbitals, *J. Phys. Chem.*, 1995, **99**, 9352-9362.
- 12 D. Y. Zubarev and A. I. Boldyrev, Developing paradigms of chemical bonding: adaptive natural density partitioning, *Phys. Chem. Chem. Phys.*, 2008, **10**, 5207-5217.